Modeling Estuary-Scale Climate Change: Narragansett Bay Under RCP 8.5

Jonathan Benoit

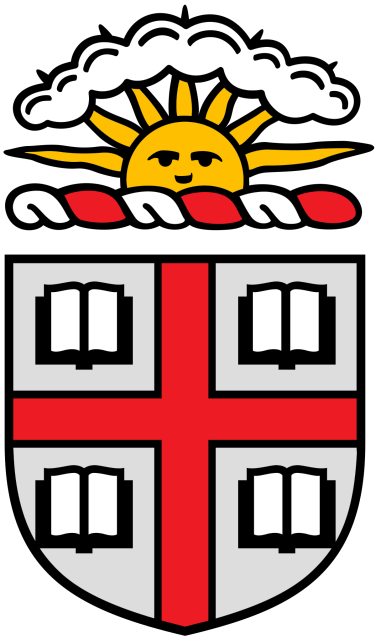

Advisor: Baylor Fox-Kemper

Department of Earth, Environmental and Planetary Sciences
Brown University
May 2022

1 Abstract

Global climate simulations have made predictions about how Earth's oceans and atmosphere will change over the remainder of this century with climate change; however, their coarse resolution leaves many coastal regions, such as smaller estuaries, unresolved. This work uses the output from a global climate simulation to force the Ocean State Ocean Model (OSOM)—a local (200 meter resolution) coastal ocean model for Narragansett Bay and nearby coastal regions—to simulate pre-industrial (1917), modern (2018), and future (2100) conditions as predicted by the RCP 8.5 emissions scenario, which assumes no mitigation of anthropogenic greenhouse gases. Measured changes in the northwestern Atlantic Ocean have well exceeded the global average in terms of surface warming and sea level rise, and models predict greater changes to come with increasing salinity, in addition to temperature and sea level, due to changing dynamics between the Gulf Stream and Labrador Current. Comparison between the three simulated years indicates that warming is spatially heterogeneous with waters close to shore warming up to 0.4 °C more than the regional average indicated by global models from 1917-2100. Regional salinity increases in the region are also found to have a significant impact within Narragansett Bay as near-river salinity increases by up to 3 psu between 1917 and 2100. These changes correlate with density and velocity changes in the estuary with waters becoming less dense on average and median velocity magnitudes decreasing by 7% from 1917 to 2100. The effect of sea level rise is significant with approximately 1.0 meter of sea level rise from 1917 to 2010, the average low tide in 2100 nearly reaching the level of the average high tide in 1917, and tidal amplitude decreasing. OSOM is also used to simulate the effects of thermal effluent from the former location of the Brayton Point Power Station to understand how the heat anomaly from the power station compares to climate warming. While the average temperature anomaly in the region has matched the surface warming in Narragansett Bay overall, tidal effects are shown to be significant in thermal plume extent over daily timescales and the thermal plume becomes weaker with depth.

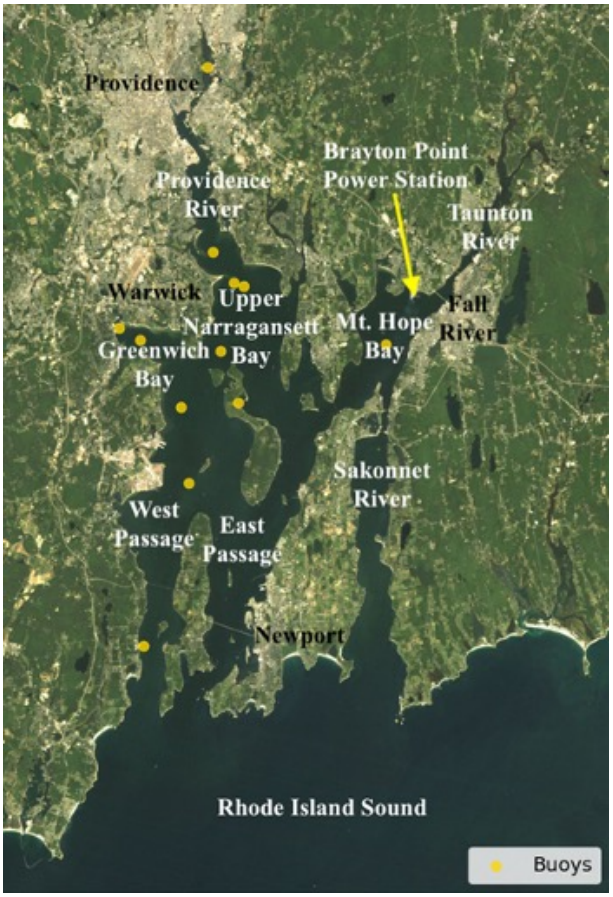

Figure 1: Satellite scene of Narragansett Bay with labeled regions and location of buoys (Benoit and Fox-Kemper 2021).

2 Introduction

Ocean physics set the stage for marine, terrestrial, and estuarine ecosystems as well as the human societies that depend on these ecosystems by controlling temperature, salinity, and nutrient availability within the water and weather and climate experienced on land. Narragansett Bay (Figure 1) and nearby coastal waters, specifically, provide a habitat for a diverse assemblage of organisms, providing a growing source of food for humans and other terrestrial species (Hale, Hughes, and Buffum 2018, Byron et al. 2011). Humans alter Narragansett Bay through the release of nutrients from wastewater treatment plants and agricultural runoff—implicated in Narragansett Bay hypoxia—as well as through the concentrated release of heat from power plants and other, more widespread, forms of pollution (Deacutis et al. 2006, Benoit and Fox-Kemper 2021). On longer timescales, Narragansett Bay has become warmer and sea level has risen due to anthropogenic climate change at a rate many times faster than the global average. Climate change will continue to dramatically impact the northwestern Atlantic over the next century, so a detailed understanding of how these changes impact smaller scales is critical towards mitigation and adaptation. This work investigates how regional scale climate changes over the timescale of centuries manifest in local scale oceanography that affect humans, organisms, and ecosystems directly.

2.1 Narragansett Bay Circulation

On sub-daily timescales, Narragansett Bay flow is dominated by diurnal tides causing variability in temperature, salinity and other parameters. The balance between fresh river flow at the surface and salty oceanic flow at depth sets up estuarine circulation that works to stratify the estuary between a fresh surface and salty bottom; however, Narragansett Bay's shallow depth means that wind-driven mixing can often penetrate deeply enough to de-stratify, primarily in winter (Geyer and MacCready 2014). Averaged over days, the tidal flow results in net transport from rivers in the north to the Atlantic Ocean in the south as tracers are flushed out of Narragansett Bay over the timescale of about 14-17 days in summer and about 31-33 days in winter (Sane et al. 2020). This distinct seasonality in flushing time reflects changes in evaporation, precipitation, air temperature, winds, and radiative heat fluxes for each season, resulting in warm, stratified summer conditions and cold, well-mixed winter conditions. River input peaks in the winter and spring due to precipitation seasonality and shallower embayments tend to experience greater temperature extremes than deeper regions due to their lower heat capacity (Fisher and Mustard 2004). Narragansett Bay and its ecosystems respond to interannual variability in the atmosphere and the northwestern Atlantic as well as variations in human behavior relating to pollution and fishing practices. Changes over decades to centuries have been measured with waters becoming warmer and sea levels rising in and around Narragansett Bay while global climate projections predict dramatic change by the end of the current century (Shearman and Lentz 2010, Oppenheimer et al. 2019). Climatic changes makes the baseline for shorter term cycles non-static.

2.2 Climate Change Globally

Global-scale climate models have refined our understanding of how climate change will affect the oceans and atmosphere by the end of the century. These models have shown that the primary uncertainty in the future of Earth's climate is the role of humans through the release of greenhouse gases (Oppenheimer et al. 2019). Representative Concentration Pathways (RCPs) were designed to capture how different greenhouse gas emissions pathways would impact Earth's climate response. RCP 8.5 represents the pathway with the largest greenhouse gas emissions, corresponding to a scenario with no climate mitigation policies, slow technological growth, and high population growth starting in 2006 (Riahi et al. 2011). Other RCPs assume that emissions peak, then decline, sometime during this century with RCP 6, RCP 4.5, and RCP 2.6 assuming peak emissions in the 2080s, 2040s, and 2020s, respectively. RCP 2.6 limits global warming to 2 °C above pre-industrial levels, the long-term temperature goal set by the Paris Agreement with a preference for 1.5 °C. The forcing data used in this work uses RCP 8.5 projections. This scenario provides a good benchmark for what risks to prepare for as the patterns of climate change are expected to be similar, though smaller in magnitude, for lower emission scenarios.

Regional climate information is available from the latest Intergovernmental Panel on Climate Change (IPCC) assessment reports (IPCC 2021). The Interactive Atlas (Gutiérrez et al. 2021) and a sea level projection tool co-produced by the IPCC and NASA are useful resources for accessing these assessed data (`https://sealevel.nasa.gov/ipcc-ar6-sea-level-projection-tool`).

In addition to predicting the future, climate models utilizing data assimilation provide a clearer view of the climate change that has already occurred by filling in gaps from past observations. Since pre-industrial times, the Earth has gotten warmer and wetter on average with the greatest impacts in the Arctic (Oppenheimer et al. 2019). These changes are expected to continue independent of greenhouse gas reductions as most Earth systems can take decades to centuries to equilibrate with anthropogenic forcing, and even longer for

slow-to-respond systems such as the deep ocean and ice sheets that contribute to sea level (Fox-Kemper et al. 2021).

2.3 Climate Change in the Northwestern Atlantic

Though global climate change is framed in terms of mean atmospheric temperature change such as 2 °C above pre-industrial levels as predicted by RCP 2.6, changes on local scales can be far greater, especially in regions where anthropogenic changes put in motion local feedback mechanisms such as sea-ice albedo feedback or in places where major circulation patterns are altered.

Climate change is expected to impact the northwestern Atlantic like few other regions of the world, with temperatures warming at a rate up to three times faster than the global sea surface temperature trend (MERCINA Working Group et al. 2015, Saba et al. 2015, Dupigny-Giroux et al. 2018, Neto, Langan, and Palter 2021). Near and within Narragansett Bay, long-term instrumental and palaeoceanographic records indicate that the region has warmed at a rate of 0.06–0.26 °C/decade in the past century (Shearman and Lentz 2010, Salacup et al. 2019, Smith, Whitehouse, and Oviatt 2010), while satellite-derived surface temperature records have shown a warming of 0.5–1.2°C from 1984-2021, putting the current rate of warming at 0.23 ± 0.1°C/decade (Benoit and Fox-Kemper 2021). Projecting the observed warming trends assuming a constant rate of temperature increase over the next century results in 1.8 ± 0.8°C of warming by 2100 according to the recent trend by satellites and 1.28 ± 0.8°C of warming from the longer-term records. However, climatic warming is known to be accelerating, so the current rate derived from satellites overestimates warming over the last century and underestimates warming over the next.

According to the International Laboratory for High-Resolution Earth System Predition's (iHESP) RCP 8.5 climate simulation, total sea surface temperature warming along the coast of the Northeastern US from the early 20th century to the end of the 21st century is projected to outpace 99% of other ocean regions (Figure 2). Ecosystem responses to this dramatic warming have been documented already in the case of cod fishery collapse and amplified lobster blooms in the Gulf of Maine (Pershing et al. 2015, Goode et al. 2019). Salinity is also predicted to increase in this region more than 98% of other ocean regions (Figure 3). The projected changes follow similar spatial patterns to the changes over the past century, as indicated by iHESP's data-assimilated hindcast runs. The main mechanism behind these dramatic regional changes has to do with the interplay between the northward flow of the Gulf Stream, carrying warm, salty water from the Gulf of Mexico and the Labrador Current, carrying cold, fresher water from the Arctic. Current circulation involves the Gulf Stream peeling away from the eastern coast of the United States near the mid-Atlantic states and subsequent flow towards Europe. The Labrador Current flows southward from the Arctic to fill in the rest of the coastal waters north of where the Gulf Stream splits off (Figure 4). Models agree that polar amplification of warming in the Arctic source of the Labrador Current and strong atmospheric warming play a role in the large regional changes in the northwest Atlantic, though a consensus has not been reached about the potential role of a weakening Atlantic Meridional Overturning Circulation (AMOC), northward shifts in the Gulf Stream, retreat of the Labrador Current, or increased Gulf Stream eddy formation (Saba et al. 2015, Alexander et al. 2020). For iHESP's RCP 8.5 simulations and the analysis in this work, the Gulf Stream does move further north, causing the large salinity—in addition to temperature—increases in the region.

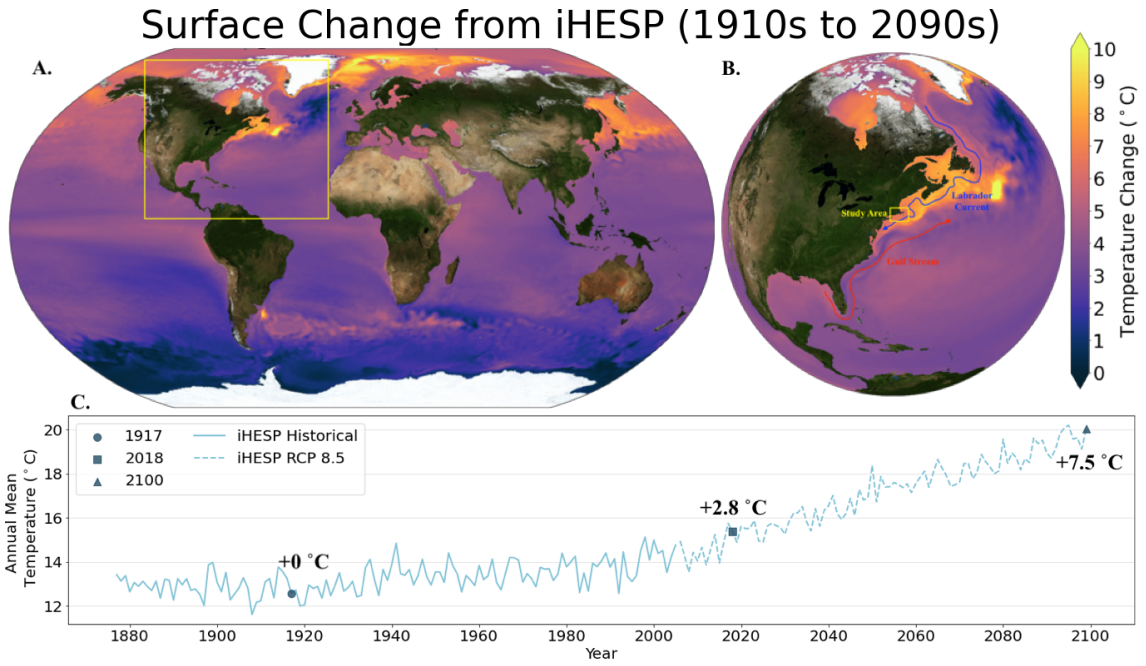

Figure 2: Global (A) and northwest Atlantic (B) sea surface temperature (SST) change as predicted by iHESP between the 1910s and 2090s with a regional timeseries (C) on the coastal shelf near Narragansett Bay. The SST values for the three simulation years used in this study are marked on the timeseries.

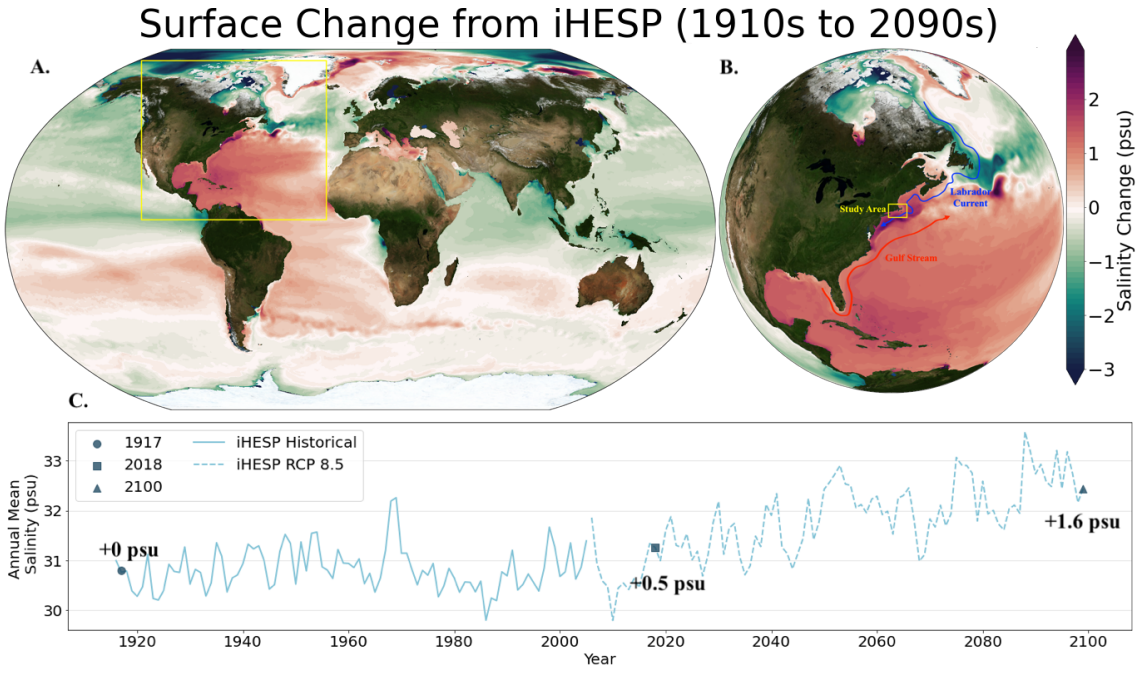

Figure 3: Global (A) and northwest Atlantic (B) sea surface salinity (SSS) change as predicted by iHESP between the 1910s and 2090s with a regional timeseries (C) on the coastal shelf near Narragansett Bay. The SSS values for the three simulation years used in this study are marked on the timeseries.

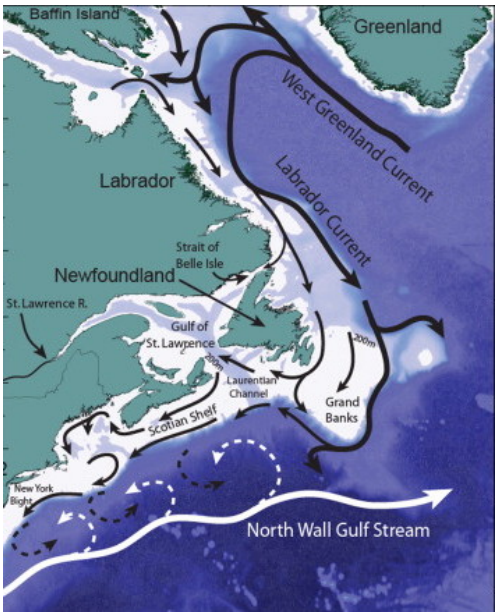

Figure 4: Large scale ocean circulation in the Northwest Atlantic (Townsend et al. 2010). Circulation is dominated by the Gulf Stream bringing warm, salty water from the south and the Labrador Current, bringing cold, fresher water from the Arctic. The balance between these ocean currents is expected to change over the next century, causing large temperature and salinity increases near the coast of New England.

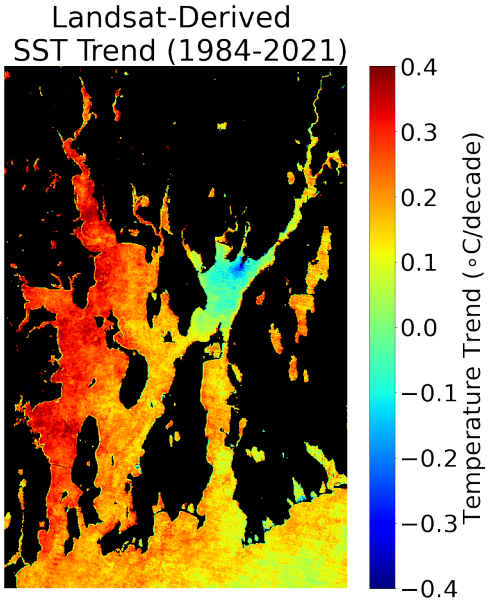

Figure 5: Surface temperature trend (1984-2021) in Narragansett Bay as measured by the Landsat satellite series (Benoit and Fox-Kemper 2021). Warming in the region is heterogeneous with large scale warming (0.23 ± 0.1 °C/decade) overall, local cooling (-0.38 ± 0.1 °C/decade) near where thermal effluent from the Brayton Point Power Station was removed, and near zero (-0.02 ± 0.1 °C/decade) cooling averaged over Mt. Hope Bay.

Narragansett Bay warming, as measured by satellites, show spatial heterogeneity with strong positive warming in the region overall, significant cooling near where the thermal effluent from the Brayton Point Power station was removed, and a net zero change in Mt. Hope Bay overall (Figure 5, Benoit and Fox-Kemper 2021). Net zero warming in Mt. Hope Bay means that the ecology of the region has experienced a similarly sized temperature anomaly as what the rest of the estuary now experiences due to climate warming on average. Much of the analysis done on this effluent was inferred from satellite-derived surface temperature, which does not resolve sub-monthly plume behavior or depth. This work produces hourly simulations of the plume dynamics in three dimensions. Understanding the extent to which the thermal plume made this region a good analog for climate warming may allow us to understand how much to infer from Mt. Hope Bay about heat-induced ecological effects for the rest of Narragansett Bay as temperatures continue to rise.

2.4 The Ocean State Ocean Model (OSOM)

Modeling of ocean systems applies our best knowledge of fluid mechanics to simulate past and future conditions in the ocean. The Ocean State Ocean Model (OSOM, Figure 6) is an application of the Regional Ocean Modeling System (ROMS) to Narragansett Bay and Rhode Island Sound. Past iteration of OSOM have been compared to in-situ measurements of temperature and salinity using buoy measurements as well as satellite-derived surface temperatures (Sane et al. 2020). Comparison to buoy data shows that OSOM accurately simulates high frequency variability on the timescale of tidal cycles, but averaged data shows biases of up to 5 °C (Sane et al. 2020). Satellite comparison shows good correspondence within measures of uncertainty when spatially averaged, though model temperature seasonality exceeds seasonality measured by Landsat by approximately 1 °C (Figure 7). The use of OSOM to predict climatic change does not require a perfectly realistic model because the focus here is on differences between model runs and model biases are expected to be similar for each simulation based on the similarities in model setup.

OSOM has been applied to modern seasonal and interannual timescales, but this work presents the first successful attempt to use OSOM to simulate climatic changes in Narragansett Bay on the timescale of the next century and to provide a pre-industrial reference. This assessment provides the highest resolution look yet at how the estuarine-dynamics of Narragansett Bay and Rhode Island Sound may change under rapid climate change.

3 Methods

Conditions in Rhode Island coastal waters are simulated for three full years representing pre-industrial (1917), modern (2018), and future (2100) conditions. These years were chosen because 1917 and 2100 were the earliest and latest dates of available data and 2018 has been simulated with OSOM in the past, allowing for inter-model validation. The surface and boundary forcing data come from iHESP's High-Resolution (10 km) CESM. Model data earlier than 2006 represent a data-assimilated hindcast simulation, while later data are predictions based on RCP 8.5 climate forcing. Relevant atmospheric data over the OSOM region are extracted from the iHESP dataset to force the model for each of the three years, and ocean data from iHESP provide open-ocean boundary conditions for the model. The OSOM configuration remains the same as previous implementations of OSOM in terms of physical parameterization (Sane et al. 2020), though some flags in OSOM are changed to best suit the available forcing data.

Figure 8 provides a summary of the differences between the three simulation years in terms of the scalar forcing variables. Air temperature, sea surface temperature, salinity, precipitation and sea surface height all

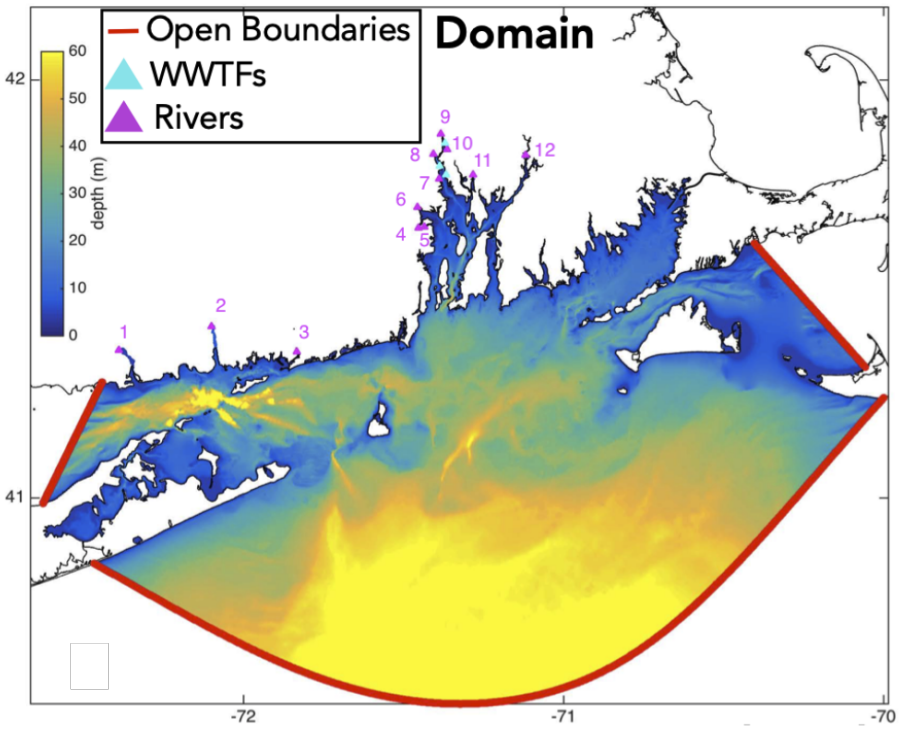

Figure 6: Domain of the Ocean State Ocean Model (OSOM) showing bathymetry (Sane et al. 2020). The model is forced by a surface atmospheric boundary, open ocean boundaries (red), and input from rivers (magenta). Wastewater treatment facilities (WWTFs), which impact nitrogen-input and hypoxia, are marked in light blue.

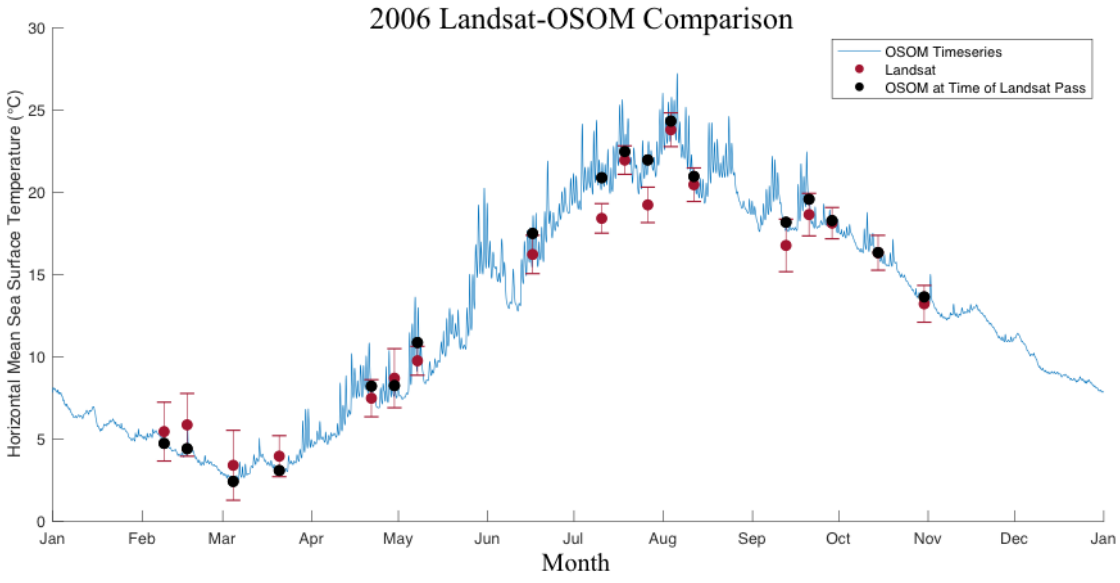

Figure 7: Comparison of OSOM to Landsat data for a 2006 OSOM simulation year.

increase over time according to iHESP's past and future simulations, with future changes exceeding past changes under RCP 8.5. All of the variables for the three years selected, except for precipitation, reflect subsequent increase consistent with these long term changes with 7.9°C warming in the atmosphere, 7.7°C warming in the ocean, 2.1 psu increase in salinity, and 1.0 m increase in sea surface height from 1917-2100. For precipitation, the 2018 case has the greatest rainfall while the 2100 case has an intermediate amount between 2018 and 1917, reflecting the 2100 simulation year being an anomalously dry year for the end of the century; however, precipitation still increases by 4.2×10^{-3} kg m/s from 1917 to 2100.

Figure 8: Comparison of the scalar parameters used to force OSOM for each simulation year. Numbers on the x-axis represent the average change between 1917 and 2100.

3.1 Atmospheric Forcing

The atmosphere exchanges heat, moisture, and kinetic energy with the ocean, so atmospheric variables must be specified to simulate the atmospheric exchanges in OSOM. Surface atmospheric values taken from iHESP data for 1917, 2018, and 2100 specify this forcing for air temperature, humidity, pressure, and winds. The temperature, humidity, and wind data are represented by daily averages while pressure data varies every six

hours. The spatial resolution of atmospheric forcing variables is 10 km; though, the temperature, humidity, and pressure values are averaged over the region to minimize large variations when OSOM calculates longwave heat fluxes and to match previous OSOM runs that assumed a homogenous atmosphere in these variables. Wind variables vary over the domain at the 10 km resolution.

Further surface forcing includes shortwave (solar) radiation and longwave radiation. Shortwave radiation is assumed to not change between the three comparison years as changes in the Earth's orbit should not induce significant changes in solar radiation over a year and interannual solar variations are not the subject focus. Daily average shortwave data from 2005 forces all three simulation years. OSOM determines day-night variations in shortwave radiation from daily average data and the model's latitude with the activation of the DIURNAL_SRFLUX flag. Longwave radiation values are calculated internally by OSOM by defining the bulk fluxes option, which computes longwave heat fluxes from forcing-specified air temperature, humidity, cloud fraction, and internally-calculated sea surface temperature according to a formulation from Berliand 1952. Cloud fraction is assumed to be zero for all times because of limited cloud data, which eliminates meteorological effects on solar radiation in these simulations.

3.2 Boundary Conditions

In addition to having atmospheric forcing at the surface, OSOM is also bounded in temperature, salinity, velocity, and sea surface height by open ocean boundary conditions to the south, east, and west as well as bounded in temperature, salinity, and volumetric flow rate by rivers to the north. Tidal effects are calculated internally based on the model time and orbital mechanics relating to the proximity of the Moon and Sun.

Available depth-varying iHESP ocean data has a 10 km horizontal resolution and varies monthly while surface data is available daily. The monthly-resolved depth profiles in temperature and salinity are adjusted within the boundary layer to meet the daily surface values. Adjustments sometimes extend below the boundary layer to ensure stable density profiles. Velocities are shifted uniformly at all depths to ensure that the average monthly profiles match at the surface to daily surface values. Sea surface height data varies daily and is adjusted by adding global mean sea level rise values from past measurements and RCP 8.5 projections taken from the Intergovernmental Panel on Climate Change's (IPCC) Sixth Assessment Report (AR6). These values are -14.2 cm for 1917, 5.2 cm for 2018, and 76.8 cm for 2100. Though sea level rise is significant for this analysis, wetting and drying is not enabled for these simulations, meaning that rising waters are not allowed to extend horizontally over formerly dry pixels. Restricting waters to pixels that are wet today means that the effect of expanding coastlines on the flow of the estuary are not considered.

River forcing matches river forcing from a previous OSOM simulation of 2018. Data for temperature and flow rate are taken from in-situ measurements and assumes that river salinity is zero. To make data for 1917 and 2100 consistent with climatic warming, river temperature was adjusted so that the mean difference between the southern boundary condition in temperature and the mean river temperature matched that of 2018 while maintaining the same seasonal variation and amplitude. This assumption is imposed on the model, so temperature near rivers will reflect this assumption independent of other external forcing.

To simulate the effect of thermal effluent, a separate 2018 simulation includes an additional river at the former location of the Brayton Point Power Station with temperatures maintained at 7 °C above other river temperatures for the 2018 case and volume flux equaling one billion gallons daily, matching temperature and volume estimates from the EPA (United States Environmental Protection Agency 2003). Salinity of the thermal effluent should match that in Mt. Hope Bay as the water is drawn from this region. The buoy data record within Mt. Hope Bay is limited to the summer, so thermal effluent salinity is estimated by

scaling salinity from a year-round buoy station near the University of Rhode Island based on the typical ratio between surface Mt. Hope Bay measurements and those at the year-round station during summer. The rest of the forcing for the thermal effluent simulation remains the same as for the 2018 case. Only winter conditions were simulated as this is a time when previous work showed the thermal anomaly from the effluent to be greatest (Benoit and Fox-Kemper 2021).

4 Results

Figure 9 summarizes the average impact of altering large scale climate forcing on local variables in Narragansett Bay as simulated by OSOM. Changes within Narragansett Bay prove to be distinct from regional changes and spatially heterogeneous over the OSOM domain as well as within the estuary.

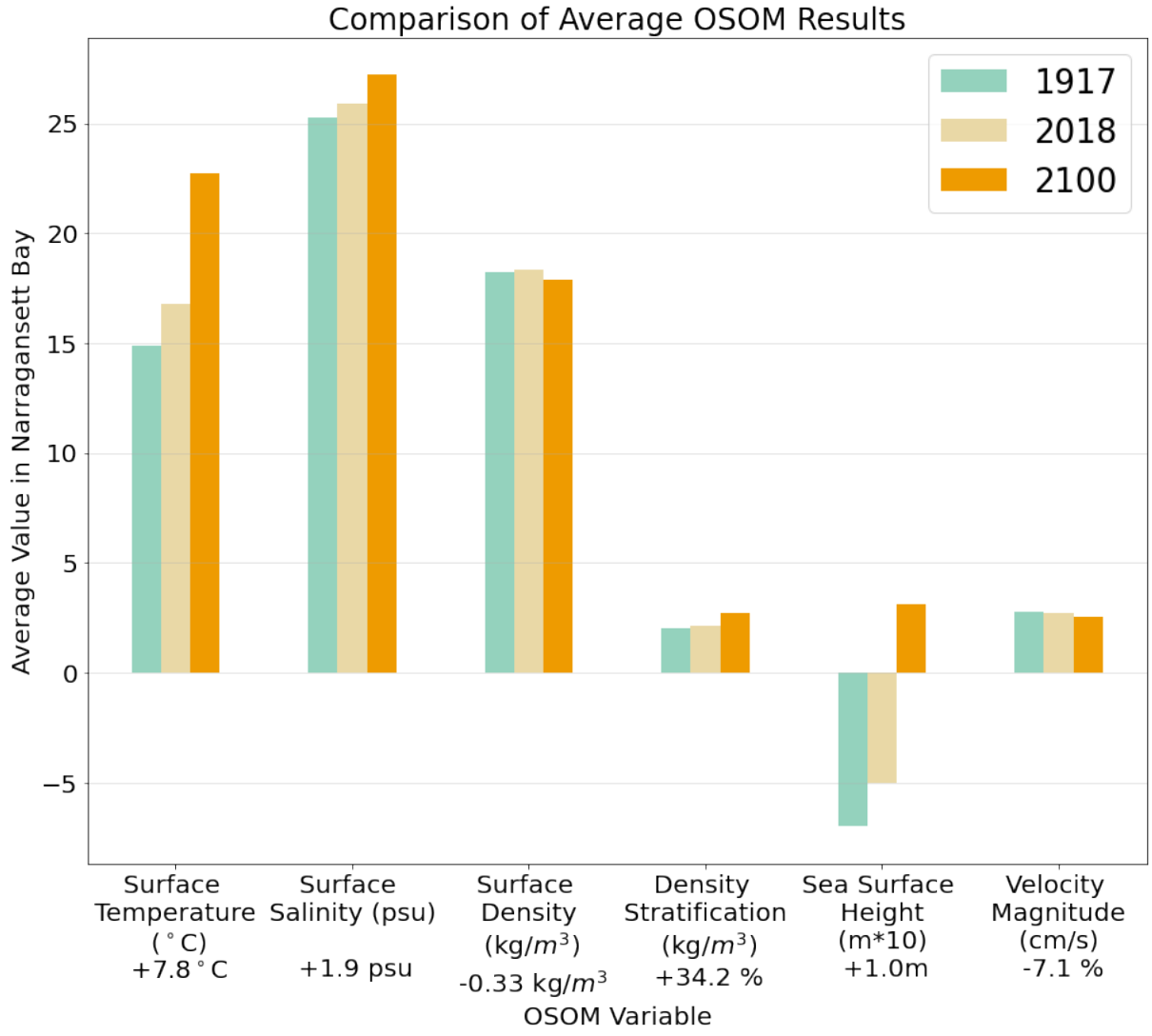

Figure 9: Resulting effects on OSOM for each of the simulation years. Numbers on the x-axis represent change from the 1917 to 2100 case.

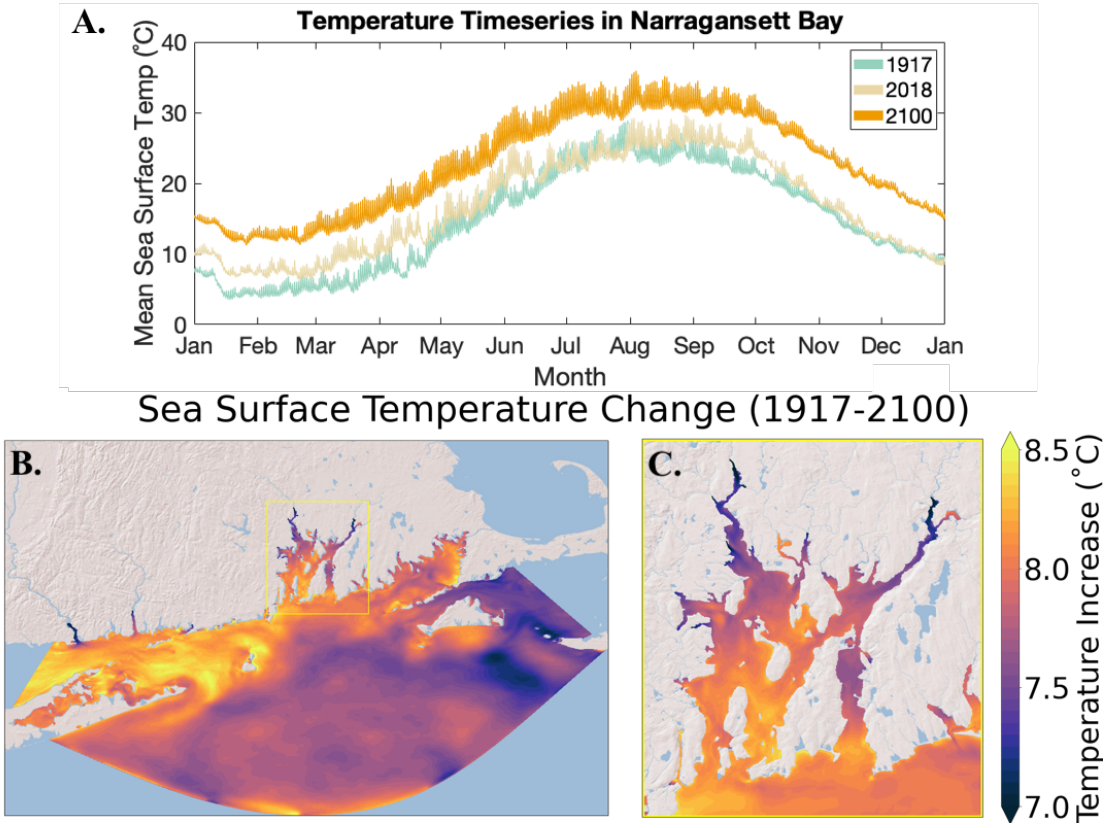

Figure 10: Sea surface temperature timeseries for each of the three simulated years (A) and mean surface temperature anomalies between 1917 and 2100 for the OSOM domain (B) and Narragansett Bay (C).

4.1 Temperature

Surface temperature follows a sinusoidal shape reflecting temperature change with the seasons. The three simulation years are offset from one another by 2.2 °C from the 1917 run to the 2018 run and by an additional 5.6 °C between the 2018 run and the 2100 run averaged over Narragansett Bay (Figure 10 A.). The surface temperature for the modern case is consistently greater than the pre-industrial case from January to April, though overlaps for much of May to December. The future case is consistently warmer than the other two cases with no overlap in any month, meaning that the coldest days in the future case are warmer than the warmest pre-industrial or present days for any given day of year. The temperature increase is large enough that temperature seasonality is shifted by up to three months in total, with the coldest (February) conditions in 2100 matching typical temperatures in May for 1917.

Average warming over the entire year proved to be spatially heterogeneous with near-shore, western regions of the OSOM domain warming up to 0.9 °C more than the domain average and warming amounts varying by up to 2.0°C (Figure 10 B.). In Narragansett Bay, warming was on average 7.8°C, which is between the 7.9°C of atmospheric warming between the pre-industrial and future years and the 7.7°C warming at the ocean boundary (Figure 10 C.). Warming varied by up to 1.7°C across the estuary and was greatest closer to the mouth, though regions further inland were closer to rivers and likely impacted by the specified river temperature.

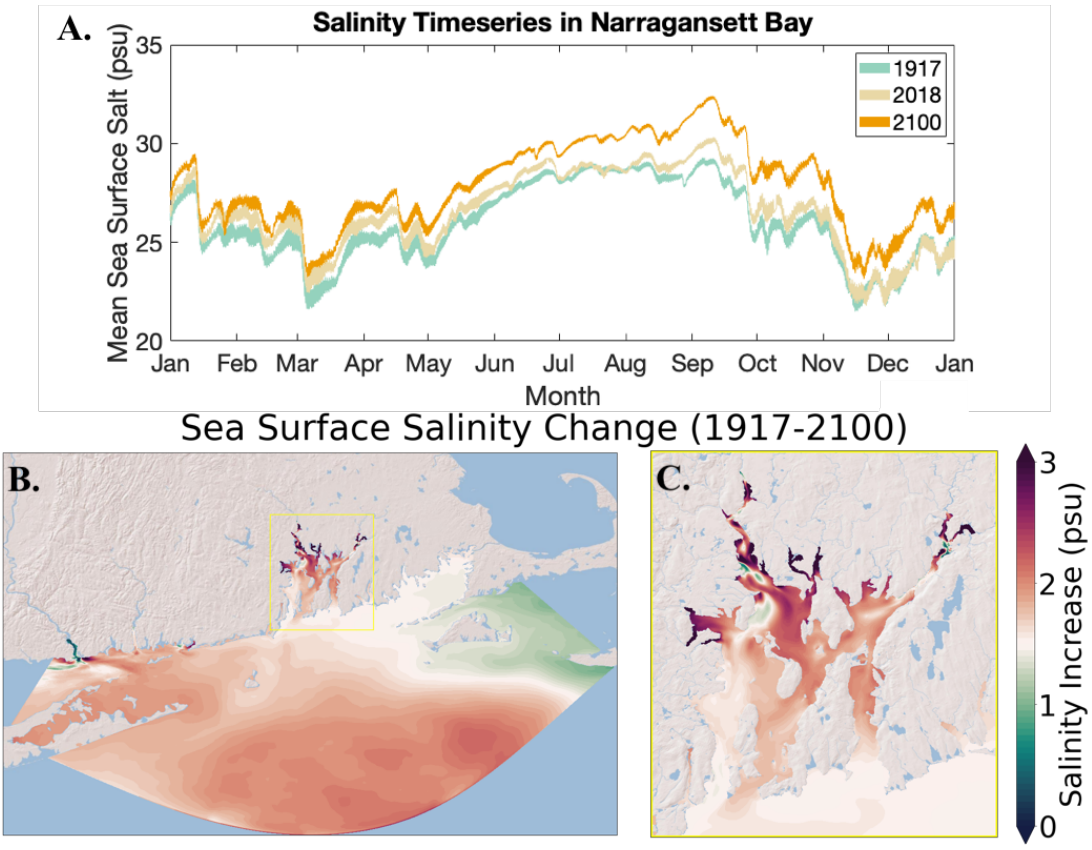

Figure 11: Sea surface salinity timeseries for each of the three simulated years (A) and mean surface salinity anomalies between 1917 and 2100 for the OSOM domain (B) and Narragansett Bay (C).

4.2 Salinity

Surface salinity seasonality primarily reflects changes to precipitation and river transport. Because the three simulation cases had the same river transport, the salinity time series follow a similar shape with greater salinity in the summer and early autumn, when river input is lowest, and lower salinity during the winter and spring as river transport is greater (Figure 11A.). The 2018 case is generally greater than the 1917 case, though there is much overlap, while the 2100 case remains consistently above the 1917 case but overlaps with the 2018 case January to April. The greatest salinity increase is with the 2100 case in the summer and early autumn.

On average, surface salinity increased 1.7 psu over the OSOM domain from the 1917 case to the 2100 case, which is 0.4 psu less of an increase than the specified salinity increase at the open ocean boundary (Figure 11B.). Within Narragansett Bay, surface salinity increased 1.9 psu with the top 1% of salinity change reaching 2.3 psu and the bottom 1% at 1.1 psu (Figure 11C.). Greatest salinity increase is furthest up the estuary and closest to rivers where salinity increases by over 3 psu.

4.3 Density

Temperature and salinity changes are expected to impact water density. In terms of a spatial average, no significant surface density anomaly changes are found for the majority of the year in Narragansett Bay,

though average surface density is lower in the 2100 case than the other two cases for May through August by up to 3 kg/m^3 (Figure 12 A.). The surface density anomaly change varies over space with a slightly negative density trend from 1917 to 2100 for the OSOM domain (-0.59 kg/m^3) and Narragansett Bay (-0.33 kg/m^3, Figure 12 B.,C.). Narragansett Bay's lower decrease is due to the density increase (up to 3.3 kg/m^3) in waters close to rivers, where salinity increases are most significant.

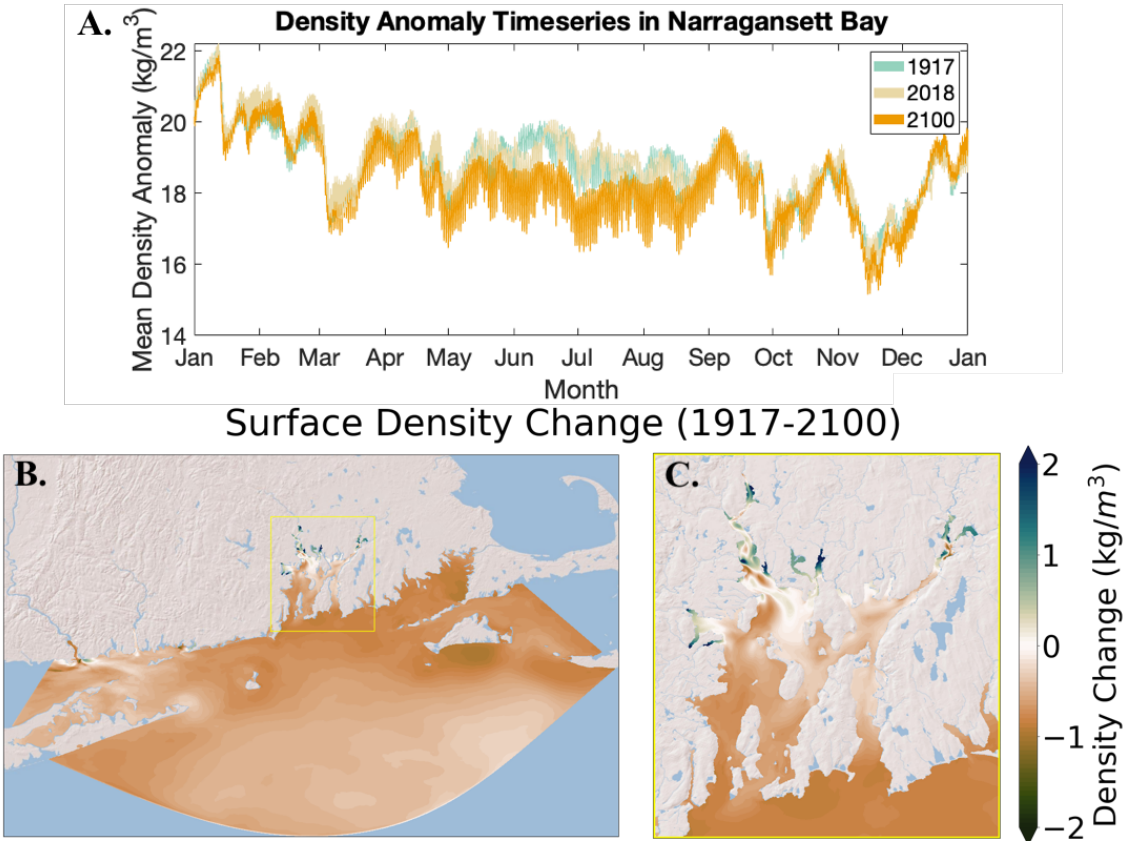

Figure 12: Sea surface density timeseries for each of the three simulated years (A) and mean surface density anomalies between 1917 and 2100 for the OSOM domain (B) and Narragansett Bay (C).

Density stratification, defined as the absolute difference between the surface and bottom density, is an important indicator of vertical mixing rates. Density stratification increases by 0.11 kg/m^3 (6%) from 1917 to 2018 and by 0.65 kg/m^3 (33%) from 2018 to 2100 over the whole domain with Narragansett Bay increases totaling 0.10 kg/m^3 (5%) from 1917 to 2018 and 0.59 kg/m^3 (37%) from 2018 to 2100. Regions closer to land experienced the greatest density stratification increase with the 99th percentile of pixels reaching a 242% increase in density stratification with the bottom one percent of pixels at a 6% increase (Figure 13). Within Narragansett Bay, the top 1% of data reaches up to a 620% increase in density stratification with the bottom 1% at a 0.1% increase.

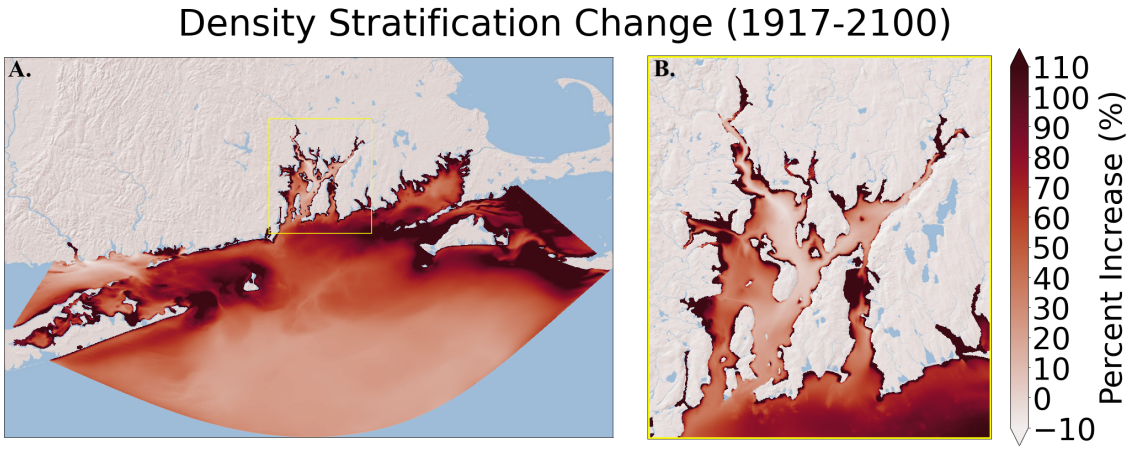

Figure 13: Maps of mean density stratification changes between the 1917 case and 2100 case for the OSOM domain (A) and Narragansett Bay (B).

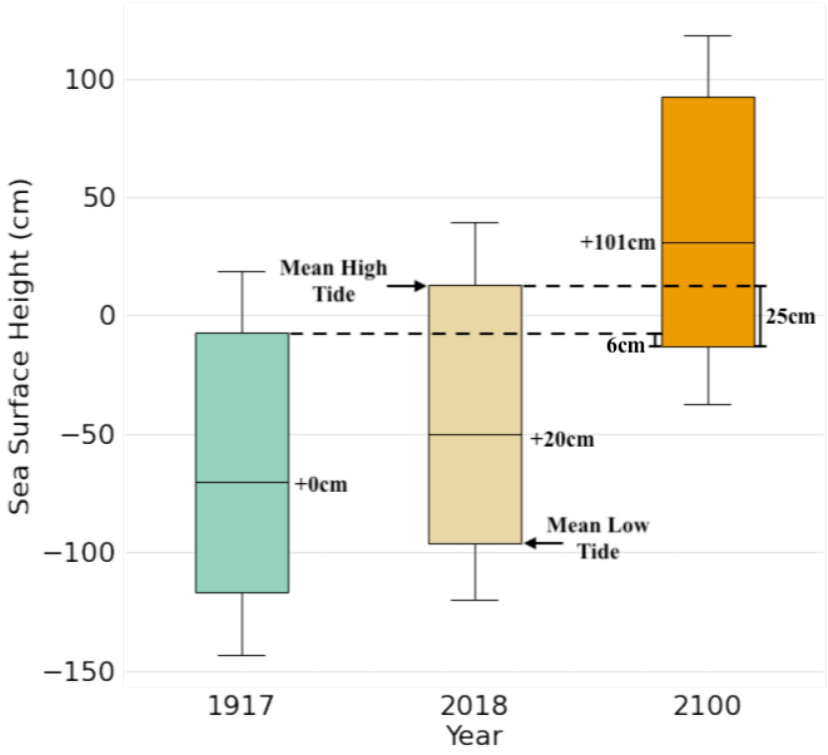

Figure 14: Mean sea surface height in Narragansett Bay for each simulation. The central bars represent the median sea surface height over the whole year while edges of the boxes represent the average high and low tides and the whiskers represent the height of the top and bottom 1% of the tides.

4.4 Sea Surface Height

Sea surface height variations reflect the regional sea surface height anomaly added on top of the global mean sea level rise for each simulation year, resulting in 19.9cm of sea level rise from 1917 to 2018 and an additional 81.1cm rise from 2018 to 2100 for a total of 101cm of sea level rise from 1917 to 2100, approximately equal to the differences in the sea surface height forcing data. Tidal variations cause sea surface height to vary around these values. The average Narragansett Bay high tide and low tide for each year along with the top and bottom 1% of tidal levels are compared in Figure 14. The average low tide for the 2100 simulation is only 6cm below than the average high tide for 1917 and 25cm below the average high tide for 2018. The approximately 1.0m average tidal amplitude decreased over the simulation years with a 0.8cm decrease from 1917 to 2018 and a 3.9cm decrease from 2018 to 2100, though the effect of wetting and drying was excluded.

4.5 Velocity

The magnitude of depth-averaged velocity change varies based on location (Figure 15). Within Narragansett Bay, the median pixel decreased in velocity magnitude from 1917 to 2100 by -7% while the mean pixel value increased by 11%, meaning that while most pixels decreased in velocity magnitude up to a -77% decrease, the top 1% of pixels saw large (up to 364%) increase in velocity magnitude. The changes within Narragansett Bay were consistent spatially and in median and mean trends between the 1917 and 2018 case and between the 2018 and 2100 case with the magnitude of change being greater for the future than for the past. These changes to velocity magnitude indicate that velocity changes are expected to be spatially complex, with impacts being highly local.

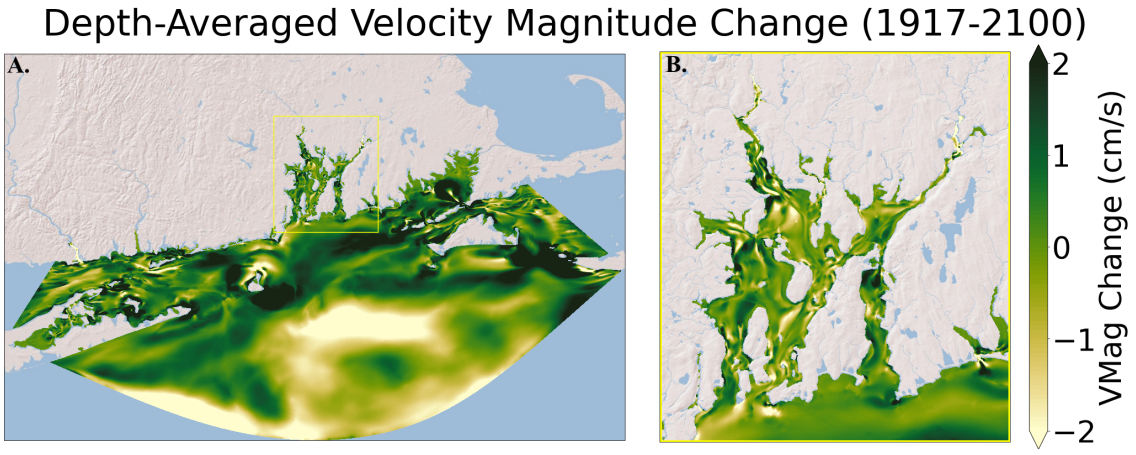

Figure 15: Maps of velocity magnitude changes between the 1917 case and 2100 case for the OSOM domain (A) and Narragansett Bay (B).

4.6 Thermal Effluent

Subtracting the winter 2018 simulation case that includes the effect of thermal effluent at the Brayton Point Power Station and the non-effluent 2018 case yields maps of temperature anomalies from the thermal effleunt in Mt. Hope Bay. The effluent causes dynamic plume behavior near Brayton Point in temperature (Figure 16). The surface temperature anomaly in Mt. Hope Bay varies significantly depending on the stage of the

tidal cycle with the anomaly concentrated near Brayton Point and the Taunton River during ebb and the extension of the anomaly into a plume as heat is advected down-estuary with the flow stage of the tide. River input truncates the thermal plume as the tide continues to go out, causing a separation between an anomaly concentrated by Brayton Point and one towards the center of Mt. Hope Bay. As the tides continue to ebb and flow, the thermal anomaly dissipates as waters continue to advect and mix. This process repeats with subsequent tidal cycles.

Figure 17 shows the accumulation of vertical temperature anomaly profiles in Mt. Hope Bay over horizontal pixels and over one day (January 1st, 2018). The average vertical profile shows a decrease in the thermal anomaly from 0.47°C at the surface to 0.23°C at the bottom, though the temperature anomaly is significant at all depths for all regions of Mt. Hope Bay on average. Individual profiles tend to follow a similar pattern of greater temperature anomaly near the surface with many profiles showing large temperature anomalies (2.0°C and greater) in the surface mixed layer.

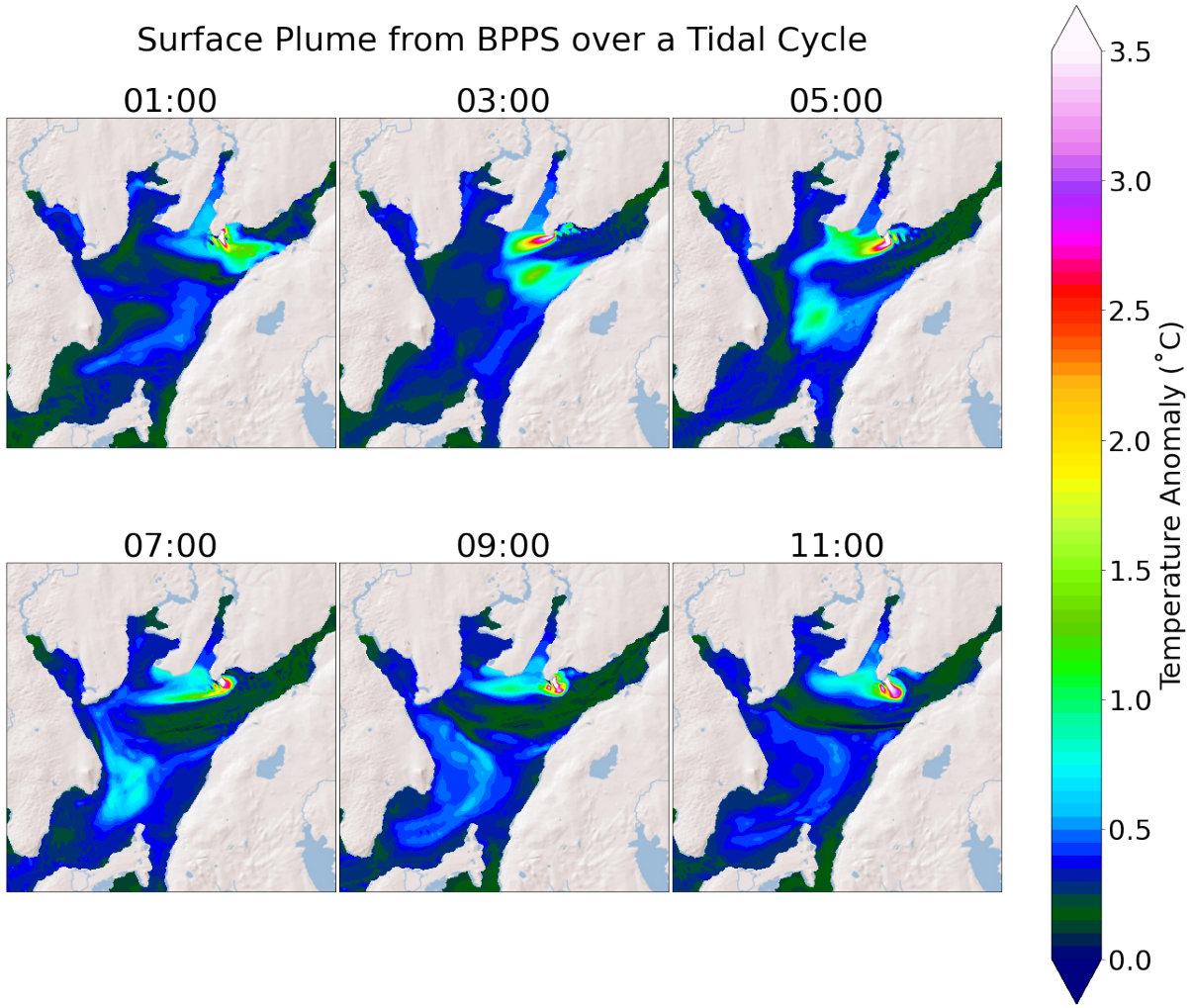

Figure 16: Timeseries of the temperature of the Brayton Point Power Station case minus the 2018 case. The timeseries shows the evolution of the thermal plume over a tidal cycle on January 1st, 2018. Temperature anomalies outside of Mt. Hope Bay were near zero.

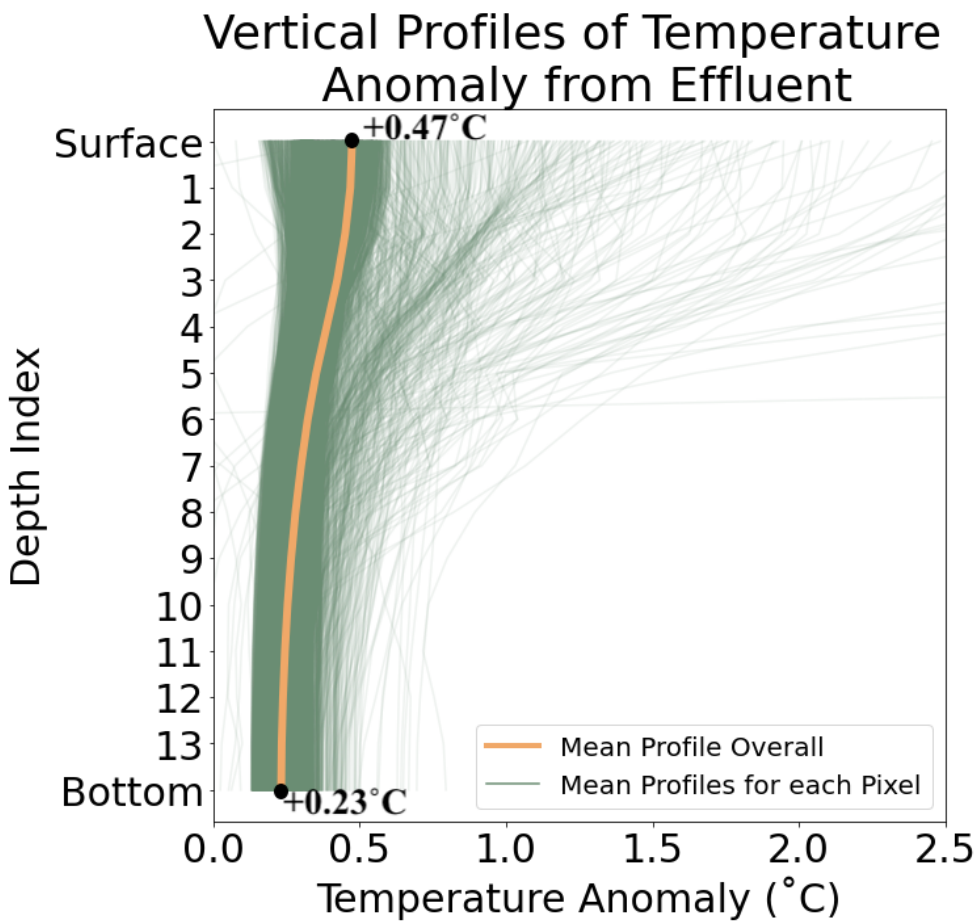

Figure 17: Vertical Profiles of the temperature anomaly in Mt. Hope Bay for the Brayton Point Power Station simulation with respect to the 2018 case for January 1st, 2018. The average vertical profile had a temperature anomaly of 0.47°C at the surface and 0.23°C at the bottom.

5 Discussion

Significant differences are found between the three climate simulation years in many of the variables important for physical oceanography, meaning that Narragansett Bay physics have been altered since pre-industrial times and is expected to experience even greater changes under rapid climate change. Though this study used forcing from RCP 8.5, the effects found can be expected to scale with lower emission scenarios. This study also only simulated three years and expects that these three years represent climatic changes because they are so distant in time; however, future work should look into simulating more years to understand how interannual variability affects these timescales.

The large increase in sea surface temperature in the region makes this region unique in its climate impacts. For Narragansett Bay, the intermediate ocean response between atmospheric warming and ocean boundary warming indicates that the role of both atmosphere-ocean heat fluxes and temperature advection are important for the climate response of temperate estuaries. The lower amount of warming near rivers indicates that the assumed relationship between river temperature and the temperature at the ocean boundary underestimates river temperature as Narragansett Bay warmed more than the open ocean. Future simulations lacking river

data should use a multi-day average of air temperature to set river temperatures more accurately.

The results for surface salinity indicate that greater salinity on the regional scale will have a local scale impact on Narragansett Bay as the along-estuary salinity gradient increases and fresher regions near rivers become more saline. These regions are expected to experience the greatest salinity increase with the largest impact being during the summer and early autumn.

Salinity and temperature both act as key environmental parameter that determines what organisms and ecosystems can exist in and near the estuary as well as key physical and chemical parameters, controlling ocean physics and chemical reactions. Increasing salinity will both impact the suitability ranges of marine organisms and test the salt tolerance of near-shore terrestrial plants. Increasing temperature will alter much of seasonal spawning and migration behavior for marine organisms, impact the ways humans recreate on the water, and make Narragansett Bay more favorable for hypoxia (Harley et al. 2006, Pörtner, Langenbuch, and Michaelidis 2005).

Increasing temperature and salinity have competing effects on density, so the impact on density is not immediately clear. It is found that the overall warming effect causes a decrease in density over the OSOM domain overall while the added effect of salinity increase in Narragansett Bay causes a smaller magnitude of density decrease within the estuary. Density increases are limited to upper regions of the rivers feeding into Narragansett Bay.

In addition to the greater hypoxic favorability from increased temperature, Narragansett Bay also is expected to undergo increased density stratification, which is an indicator of decreased vertical mixing rates, increasing the favorability of hypoxia even more. Though recent mitigation efforts have limited the nitrogen input into Narragansett Bay and reduced hypoxia in the short term, increasing the environmental favorability for hypoxia with climate change means that the sensitivity to nitrogen input will become greater in the future.

The over 1 meter of predicted total sea level rise for the region may be the most obvious impact of climate change on Narragansett Bay as coastline retreat means that beaches and shoreline properties will find themselves flooded and at greater risk of coastal erosion. Marsh ecosystem retreat currently is not keeping up with sea level rise (Raposa et al. 2016), and future changes will exacerbate the loss of marsh ecosystems. Higher sea level will also put all of coastal Rhode Island at a greater risk of flooding, especially during storm surges.

Decreasing median velocity in Narragansett Bay may somewhat mitigate coastal erosion, though velocities are expected to increase substantially in some regions while decrease in others. If Narragansett Bay is to be used as a source of renewable energy based on its strong diurnal tides, it is important to consider where velocities will change to ensure maximum efficiency.

Modeling of the Brayton Point Power Station thermal effluent provides a clearer sub-satellite observation understanding of how thermal effluents likely behaves in a temperature estuary. The tidally-driven mixing illustrates the mechanism by which the thermal effluent impacted Mt. Hope Bay and reveals that a major difference between the heat anomaly in Mt. Hope Bay and climatic warming is the stronger concentration of heat around the plume for Mt. Hope Bay compared to the more uniform warming with climate change. Further, the thermal anomaly from the plume does decrease by about half from the surface to bottom, but all depths still experience some thermal anomaly. Still, Mt. Hope Bay may be useful as a climate analogy if the differences on sub-tidal timescales and with depth are considered. This understanding can also be applied to other temperate estuaries with currently existing thermal effluent and might explain nearby organismal behavior.

All of these predicted changes to Narragansett Bay and nearby coastal regions will also have an influence

on the way the atmosphere over Rhode Island behaves, influencing what kinds of weather becomes typical. These changes as well as expanding coastlines, increasing temperature and salinity, and associated ecosystem restructuring are likely to make the Narragansett Bay of the future dramatically different from that of the past.

6 Acknowledgements

The author thanks Professor Baylor Fox-Kemper for his continued support and research expertise during this and every research project. Additional thanks goes to Aakash Sane, Rain Fan, Arin Nelson, and Paul Hall for their help in learning how to run OSOM, academic advisors Jan Tullis, Karen Fischer, and Colleen Dalton, and readers Jung-Eun Lee and Steven Clemens.

6.1 Land Acknowledgement

Narragansett Bay bears the name of the Indigenous people who first established a relationship with the estuary of focus in this study. Narragansett means "(people) of the small point of land" in Algonquian, which reflects the interdependent ties between the people and coastal waters as a resource for survival. Though much of the specifics of Narragansett Indigenous knowledge systems about Narragansett Bay may have been tragically lost through colonization, by living off the land and waters, Narragansett People developed intuitive knowledge systems about the coastal region in which they lived. One example includes the naming of the Woonasquatucket River, which means "where the salt water ends" in Algonquian. Indigenous Knowledge systems tend to be inherently relational, place-based, and empirically tested through survival context. Though the knowledge gained through the western scientific approach taken in this study only began to be applied to Narragansett Bay in the past century, people have understood much about Narragansett Bay and North America's other estuaries for thousands of years, and the knowledge gained through western quantitative methods represents advancement in only one kind of knowledge of Narragansett Bay among many.

References

Alexander, M.A. et al. (2020). "The Response of the Northwest Atlantic Ocean to Climate Change". In: *Journal of Climate* 33.2, pp. 405–428. DOI: 10.1175/JCLI-D-19-0117.1.

Benoit, J. and B. Fox-Kemper (2021). "Contextualizing Thermal Effluent Impacts in Narragansett Bay Using Landsat-Derived Surface Temperature". In: *Frontiers in Marine Science* 8.705204. DOI: 10.3389/fmars.2021.705204.

Berliand, M. E. (1952). "Determining the net long-wave radiation of the earth with consideration of the effect of cloudiness". In: *Izvestiya Akademii Nauk SSSR, Seriya Geologicheskaya* 1, pp. 64–78.

Byron, C. et al. (2011). "Calculating ecological carrying capacity of shellfish aquaculture using mass-balance modeling: Narragansett Bay, Rhode Island". In: *Ecological Modelling* 222.10, pp. 1743–1755. DOI: 10.1016/j.ecolmodel.2011.03.010.

Deacutis, C.F. et al. (2006). "Hypoxia in the Upper Half of Narragansett Bay, RI, During August 2001 and 2002". In: *Northeastern Naturalist* 13.4, pp. 173–198. DOI: 10.1656/1092-6194(2006)13[173:HITUHO]2.0.CO;2.

Dupigny-Giroux, L.A. et al. (2018). "Northeast". In: *Impacts, Risks, and Adaptation in the United States*. Vol. II. Fourth National Climate Assessment, pp. 669–742. DOI: 10.7930/NCA4.2018.CH18.

Fisher, J.I. and J.F. Mustard (2004). "High spatial resolution sea surface climatology from Landsat thermal infrared data". In: *Remote Sensing of Environment* 90.3, pp. 293–307. DOI: 10.1016/j.rse.2004.01.008.

Fox-Kemper, B. et al. (Aug. 2021). "Climate Change 2021: The Physical Science Basis. Contribution of Working Group I to the Sixth Assessment Report of the Intergovernmental Panel on Climate Change". In: ed. by V. Masson-Delmotte et al. United Kingdom and New York, NY, USA: Cambridge University Press. Chap. Ocean, Cryosphere and Sea Level Change, pp. 1211–1362. DOI: 10.1017/9781009157896.011.

Geyer, W.R. and P. MacCready (2014). "The Estuarine Circulation". In: *Annual Review of Fluid Mechanics* 46, pp. 175–97. DOI: 10.1146/annurev-fluid-010313-141302.

Goode, A.G. et al. (2019). "The brighter side of climate change: How local oceanography amplified a lobster boom in the Gulf of Maine". In: *Global Change Biology* 25.11, pp. 3906–3917. DOI: 10.1111/gcb.14778.

Gutiérrez, J. M. et al. (Aug. 2021). "Climate Change 2021: The Physical Science Basis. Contribution of Working Group I to the Sixth Assessment Report of the Intergovernmental Panel on Climate Change". In: ed. by V. Masson-Delmotte et al. United Kingdom and New York, NY, USA: Cambridge University Press. Chap. Atlas.

Hale, S.S., M.M. Hughes, and H.W. Buffum (2018). "Historical Trends of Benthic Invertebrate Biodiversity Spanning 182 Years in a Southern New England Estuary". In: *Estuaries and Coasts* 41, pp. 1525–1538. DOI: 10.1007/s12237-018-0378-7.

Harley, C.D.G. et al. (2006). "The impacts of climate change in coastal marine systems". In: *Ecology Letters* 9.2, pp. 228–241. DOI: 10.1111/j.1461-0248.2005.00871.x.

IPCC (Aug. 2021). *Climate Change 2021: The Physical Science Basis. Contribution of Working Group I to the Sixth Assessment Report of the Intergovernmental Panel on Climate Change*. Ed. by V. Masson-Delmotte et al. United Kingdom and New York, NY, USA: Cambridge University Press. DOI: 10.1017/9781009157896.

MERCINA Working Group et al. (2015). "Oceanic Response to Climate in the Northwest Atlantic". In: *Oceanography* 14.3, pp. 76–82. DOI: 10.5670/oceanog.2001.25.

Neto, Afonso Gonçalves, Joseph A. Langan, and Jaime B. Palter (2021). "Changes in the Gulf Stream preceded rapid warming of the Northwest Atlantic Shelf". In: *Nature Communications Earth & Environment* 2.74. DOI: 10.1038/s43247-021-00143-5.

Oppenheimer, M. et al. (2019). "Sea Level Rise and Implications for Low-Lying Islands, Coasts and Communities". In: *IPCC Special Report on the Ocean and Cryosphere in a Changing Climate*. Ed. by H.-O. Pörtner et al. Intergovernmental Panel on Climate Change.

Pershing, A.J. et al. (2015). "Slow adaptation in the face of rapid warming leads to collapse of the Gulf of Maine cod fishery". In: *Science* 360.6262, pp. 809–812. DOI: 10.1126/science.aac9819.

Pörtner, H., M. Langenbuch, and B. Michaelidis (2005). "Synergistic effects of temperature extremes, hypoxia, and increases in co2 on marine animals: from earth history to global change". In: *Journal of Geophysical Research* 110.C9. DOI: 10.1029/2004JC002561.

Raposa, K.B. et al. (2016). "Assessing tidal marsh resilience to sea-level rise at broad geographic scales with multi-metric indices". In: *Biological Conservation* 204.B, pp. 263–275. DOI: 10.1016/j.biocon.2016.10.015.

Riahi, K. et al. (2011). "RCP 8.5—A scenario of comparatively high greenhouse gas emissions". In: *Climatic Change* 109.33. DOI: 10.1007/s10584-011-0149-y.

Saba, V.S. et al. (2015). "Enhanced warming of the Northwest Atlantic Ocean under climate change". In: *Journal of Geophysical Research: Oceans* 121.1, pp. 118–132. DOI: 10.1002/2015JC011346.

Salacup, J.M. et al. (2019). "Alkenone Paleothermometry in Coastal Settings: Evaluating the Potential for Highly Resolved Time Series of Sea Surface Temperature". In: *Paleoceanography and Paleoclimatology* 34.2, pp. 164–181. DOI: 10.1029/2018PA003416.

Sane, A. et al. (2020). "Consistent Predictability of the Ocean State Ocean Model (OSOM) using Information Theory and Flushing Timescales". In: *JGR: Oceans*. DOI: 10.1002/essoar.10504826.1.

Shearman, R.K. and S.J. Lentz (2010). "Long-Term Sea Surface Temperature Variability along the U.S. East Coast". In: *Journal of Physical Oceanography* 40.5, pp. 1004–1017. DOI: 10.1175/2009JPO4300.1.

Smith, L.M., S. Whitehouse, and C.A. Oviatt (2010). "Impacts of Climate Change on Narragansett Bay". In: *Northeastern Naturalist* 17.1, pp. 77–90. DOI: 10.1656/045.017.0106.

Townsend, D.W. et al. (2010). "A changing nutrient regime in the Gulf of Maine". In: *Continental Shelf Research* 30.7, pp. 820–832. DOI: 10.1016/j.csr.2010.01.019.

United States Environmental Protection Agency (2003). "Clean Water Act NPDES Permitting Determinations for Brayton Point Station's Thermal Discharge and Cooling Water Intake in Somerset, MA". In.